Electronic Supplimentary Information

Supplementary Information

Binary Activated iron-oxide/SiO_2/$NaGdF_4$:RE (RE = Ce, Eu; Yb, Er) nanoparticles: Synthesis, characterization and their potential for dual T1-T2 weighted imaging

Navadeep Shrivastava,[a] Joel Garcia,[b,c] Uéslen Rocha,[d] Carlos Ospina,[e] Diego Muraca,[f] A. S. de Menezes,[a] Carlos Jacinto,[d] Angelique Louie,[b] Giorgio Zoppellaro,[g] S. K. Sharma[h]*

Affiliations:

[a]Department of Physics, Federal University of Maranhão, São Luis-MA, Brazil.

[b]Department of Biomedical Engineering, Health Sciences Drive, University of California, Davis, California 95616, USA

[c]Chemistry Department, De La Salle University, 2401 Taft Avenue, 1004 Manila, Philippines

[d]Group of Nano-Photnics and Imaging, Institute of Physics, Universidade Federal de Alagoas, Maceió-AL, Brazil.

[e]Brazilian Nanotechnology National Laboratory (LNNano), Brazilian Center for Research in Energy and Materials (CNPEM), Campinas-SP, Brazil.

[f]Institute of Physics Gleb Wataghin, State University of Campinas, , Campinas-SP, Brazil.

[g]Regional Centre for Advanced Technologies and Materials, Palacky University, Šlechtitelů, Olomouc, Czech Republic.

[h]Department of Physics, Faculty of Science & Technology, The University of the West Indies, Trinidad & Tobago.

*Corresponding author: surender.sharma@sta.uwi.edu; surender76@gmail.com

(A) Powder X-Ray Diffraction and Analysis of Rietveld refinement of Samples:

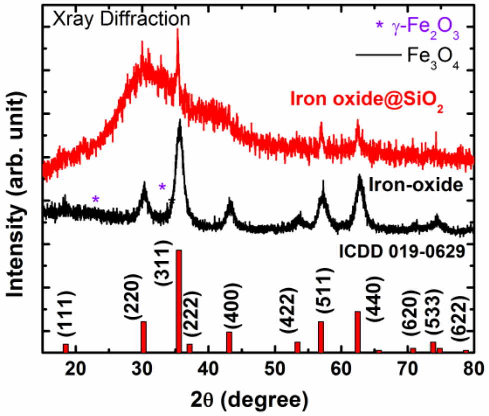

Figure S1: X-ray diffraction pattern of iron oxide (Fe_3O_4/γ-Fe_2O_3, cubic structures) nanoparticles and iron-oxide/SiO_2 seed nanoparticles.

Table T1: Table obtained from the Rietveld refinements (lattice parameters, crystallite size and concentration of phases, strain, R_{wp} and goodness of fitting (GOF)

Samples	Phases	Lattice Parameters a, b, c (Å)	Conc. (%)	D (nm)	Strain (%)	R_{wp} (%)	GOF
$NaGdF_4$	Bigger	6.0442(5), 6.0442(5), 3.6071(3)	87(2)	29(1)	0.8(1)	4.8	1.2
	Smaller	6.096(7), 6.096(7), 3.70(5)	13(2)	7.1(7)	0.07(1)		
$NaGdF_4$:Ce,Eu	Bigger	6.0529(4), 6.0529(4), 3.6086(3)	89(2)	34(1)	0.06(1)	5.1	1.2
	Smaller	6.046(8), 6.046(8), 3.64(1)	8(2)	4.5(5)	0.02(1)		
	$^*GdF_3$	6.589(5), 7.007(3), 4.390(2)	3.0(3)	53(5)	0.02		
Iron-oxide/SiO_2/ $NaGdF_4$:Ce,Eu	Pure	6.0566(6), 6.0566(6), 3.6064(4)	100	19.1(4)	0.01	4.7	1.2
$NaGdF_4$:Yb,Er	Bigger	6.0496(6), 6.0496(6), 3.6080(4)	73(2)	32(1)	0.084(5)	5.9	1.2
	Smaller	6.085(5), 6.085(5), 3.609(5)	27(2)	6.6(7)	0.01		
Iron-oxide/SiO_2/ $NaGdF_4$:Yb,Er	Pure	6.0367(6), 6.0367(6), 3.6467(6)	100	16.2(3)	0.08(1)	5.0	1.1

(B) Transmission Electron Microscopy and ESD Information:

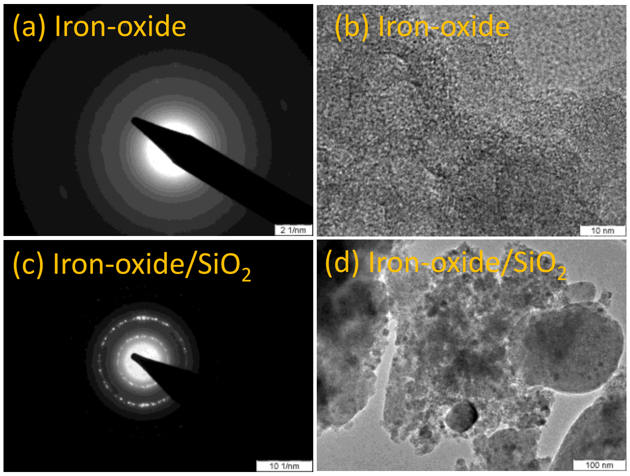

Figure S2 (i): Selected area diffraction patterns and TEM images of iron-oxide (a and b, scale 2 nm^{-1} and 10 nm respectively) and Iron-oxide/SiO$_2$ (c and d, scale 10 nm^{-1} and 10 nm respectively) nanoparticles. These experiments were performed at Philips TEM, operating at 200 keV.

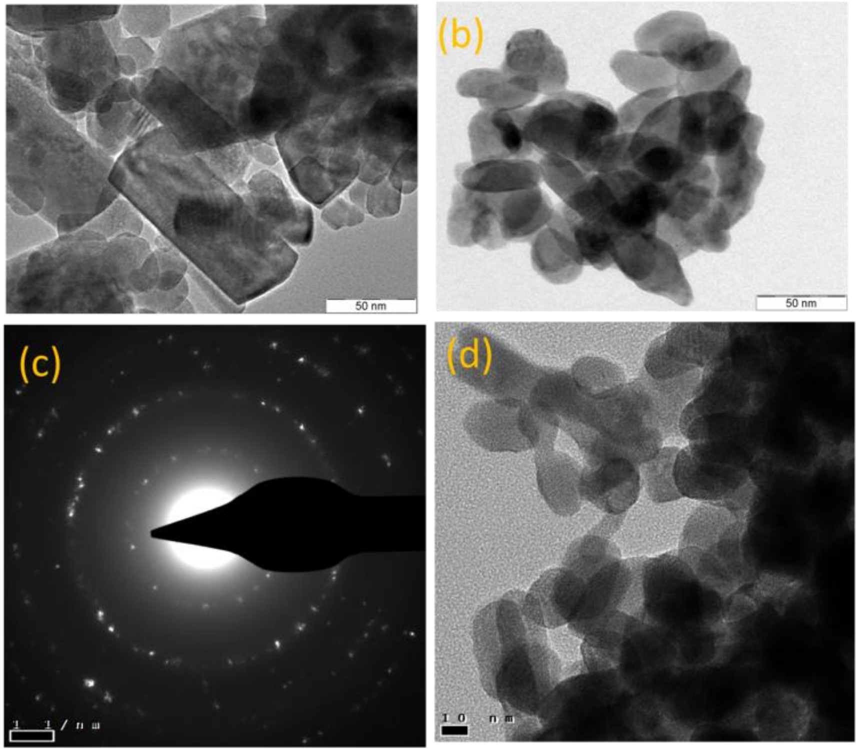

Figure S2(ii): TEM images of (a) undoped NaGdF$_4$ (scale 50 nm); (b) NaGdF$_4$:Yb,Er (scale 50 nm);; and (d) iron- oxide/SiO$_2$/NaGdF$_4$:Yb,Er nanoparticles (scale 10 nm);. (c) shows the selected area diffraction pattern for Iron- oxide/SiO$_2$/NaGdF$_4$:Yb,Er measurements (scale 1 nm^{-1});. These experiments were performed at Philips TEM, operating at 200 keV.

EDS spectra for $NaGdF_4$:Ce,Eu and iron-oxide/SiO_2/$NaGdF_4$:Ce,Eu samples have been acquired in the Titan TEM, operating at 300 keV microscope for different spots/frames. The electron beam was focused on agglomerated particles. The observed peaks confirm the existence of Fe, Si, O, Na, F, Ce, Gd and Eu elements. The Cu and C peaks may be due to copper grids of ultrathin Carbon film with Lacey Carbon. Since EDS analysis is a local measurement of small number of particles seen in the image, hence it may represent a difference in stoichiometry information. The following tables 1 and 2 show the average % elemental composition measured at different spots of the samples.

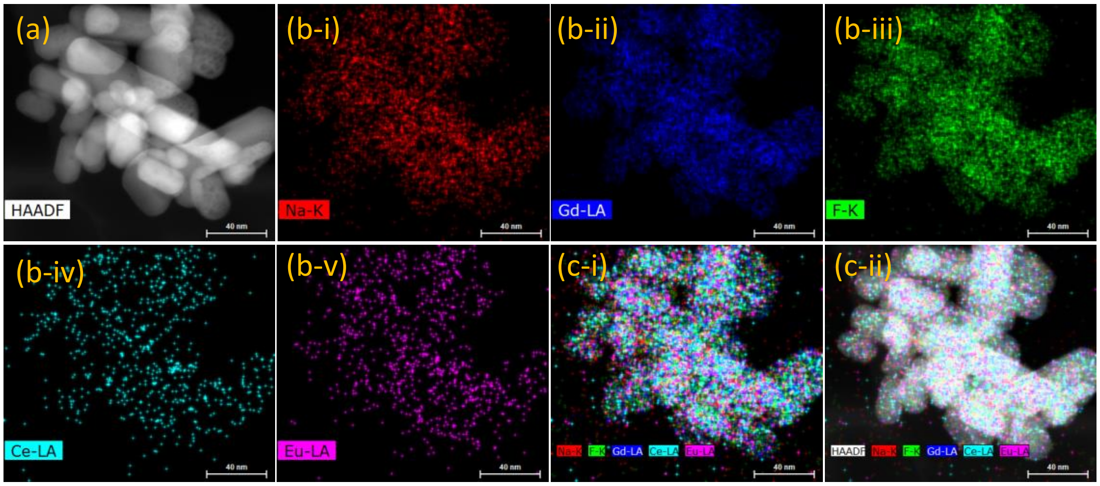

Figure S2(iii): HAADF image of downconverting $NaGdF_4$:Ce,Eu (a) EDS elemental mapping of constituent elements (b-i to b-v) and merged elemental mappings (c-i to c-ii).

Table T2. Chemical distribution of $NaGdF_4$:Ce,Eu samples.

	Spectrum 1		Spectrum 2		Spectrum 3	
Element	**Wt%**	**Wt% Sigma**	**Wt%**	**Wt% Sigma**	**Wt%**	**Wt% Sigma**
F	67.62	14.03	73.46	15.8	67.62	11.94
Na	12.48	02.21	8.63	1.17	14.03	2.32
Ce	4.27	0.44	3.74	0.42	3.38	0.39
Eu	2.04	0.25	1.97	0.23	1.64	0.20
Gd	13.56	1.05	12.20	1.01	13.23	1.06

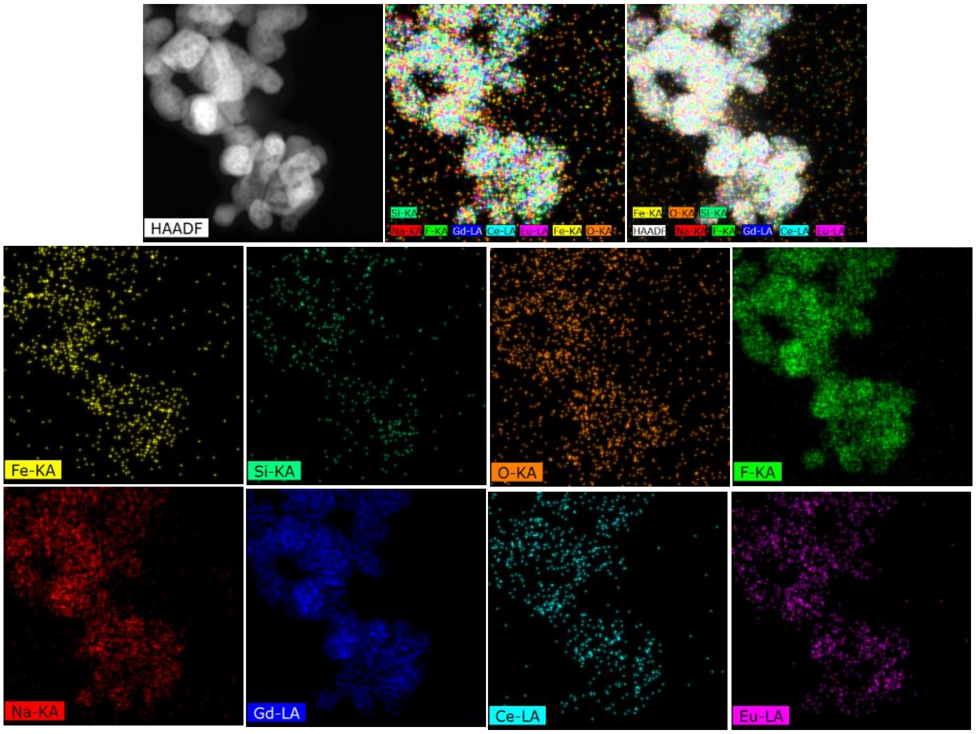

Figure S2(iv): HAADF image of magnetic downconvering iron-oxide/SiO_2/$NaGdF_4$:Ce,Eu and EDS elemental mapping of constituent elements and merged elemental mappings.

Table T3. Chemical distribution of iron-oxide/SiO_2/$NaGdF_4$:Ce,Eu samples.

	Spectrum 1		Spectrum 2		Spectrum 3	
Element	**Wt%**	**Wt% Sigma**	**Wt%**	**Wt% Sigma**	**Wt%**	**Wt% Sigma**
F	59.12	12.54	58.99	12.78	61.76	10.23
Na	13.25	12.54	11.55	2.23	10.97	1.84
Ce	1.85	0.26	2.05	0.27	2.56	0.31
Eu	1.30	0.19	1.37	0.19	1.65	0.20
Gd	11.16	1.02	11.63	1.03	13.14	1.08
Si	0.45	0.18	0.54	0.20	0.43	0.14
Fe	0.71	0.10	0.96	0.10	0.90	0.10
O	12.16	3.19	12.88	3.50	8.60	1.72

(C) ICP-AES measurements of Four Samples for Analytical Contents of Fe and Gd:

Table T4: Table for the analytical content of Fe and Gd in Samples

(Slope of Calibration Curve = 0.99999)

Samples	Fe (mg/1000 mL)	Gd (mg/1000 mL)	Sample Amount Used in 1000 mL DI water, x%HNO$_3$
NaGdF$_4$:5%Ce,5%Eu	-	6.04 ± 0.0903	124
Iron-oxide/SiO$_2$/ NaGdF$_4$:5%Ce,5%Eu	0.510 ± 0.0028)	4.65 ± 0.0294	124
NaGdF$_4$:20%Yb,2%Er	-	3.99 ± 0.0120	127
Iron-oxide/SiO$_2$/ NaGdF$_4$:20%Yb,2%Er	0.291 ± 0.009	3.51 ± 0.0181	127

(D) Photoluminescence Study:

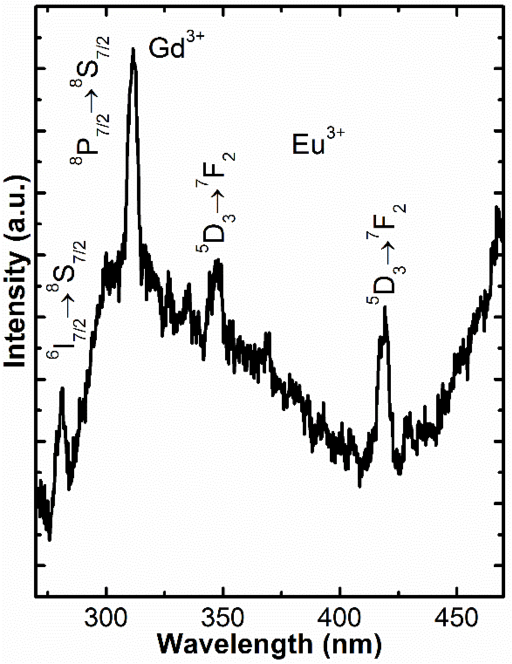

Figure S3: Emission spectrum from 275 nm to 475 nm range upon excitation by 254 nm (Ce^{3+} ions), displaying very low intensity emission lines from Ce^{3+}, Gd^{3+} and Eu^{3+} ions.

(E) UV-vis-NIR spectroscopy:

UV–vis-NIR analysis in Figure E shows the optical absorbance spectrum of the as-synthesized iron-oxide, iron-oxide/SiO_2, $NaGdF_4$:RE (RE = Ce, Eu; Yb, Er) and iron-oxide/SiO_2/$NaGdF_4$:RE nanoparticles at ambient temperature. The clear colloid obtained after 10 min sonication of nanoparticles dispersed in isopropyl alcohol (IPA) that was used as a reference sample. The spectrum shows the absorbance in the UV-visible-NIR range of the wavelength from 200 - 1700 nm. The important visible peaks originating from different samples have been tabulated in following:

Table E: Absorption peaks of the samples

S. No	Samples	Peak Positions (nm)
0.	IPA (Reference)	Only in the range of 1300 nm to 1700 nm, 222, 323, 1354, 1417, 1555, 1640
1.	Iron-oxide	**Broad Peak- 400 nm to 1100 nm**; 225, 284 **340,** 374, 1171, 1209, 1352
2.	Iron-oxide/SiO_2	222, 275, **342**, Broad peak around **378 nm**, **980,** 1133, 1169, 1208, 1353,
	RE = Ce,Eu	
3.	$NaGdF_4$:RE	223 nm, **248-257, 273**, 320, **374**, **394**, **485**, 811, 970, 1138,1172, 1213, 1354, 1550. 1637,
4.	Iron-oxide/SiO_2/$NaGdF_4$:RE	223, **250, 274, 320, 375, 432, 396, 492**, 810, 870, 970, 1638
	RE = Yb,Er	
5	$NaGdF_4$:RE	225,**272,323. 376, 481**, **824, 811,970-980**, 1056, 1138, 1171, 1217, 1339, 1355, 1550,1667,
6	Iron-oxide/SiO_2/$NaGdF_4$:RE	234, **250, 275, 320, 340, 376, 549, 970**, 810, **975**, 1138, 1206,1350, 1418, 1541, 1634

By looking the tables, it is noteworthy to mention that iron-oxide has a broad absorption band in the visible region between 400-800 nm along with characteristics absorption peaks in UV region. The emission intensity in the visible region (originating from the Er^{3+} ions when excited at 980 nm and Eu^{3+} ions, when excited at 254 nm) has been decreased (See the Figures 6 and 7 in article).

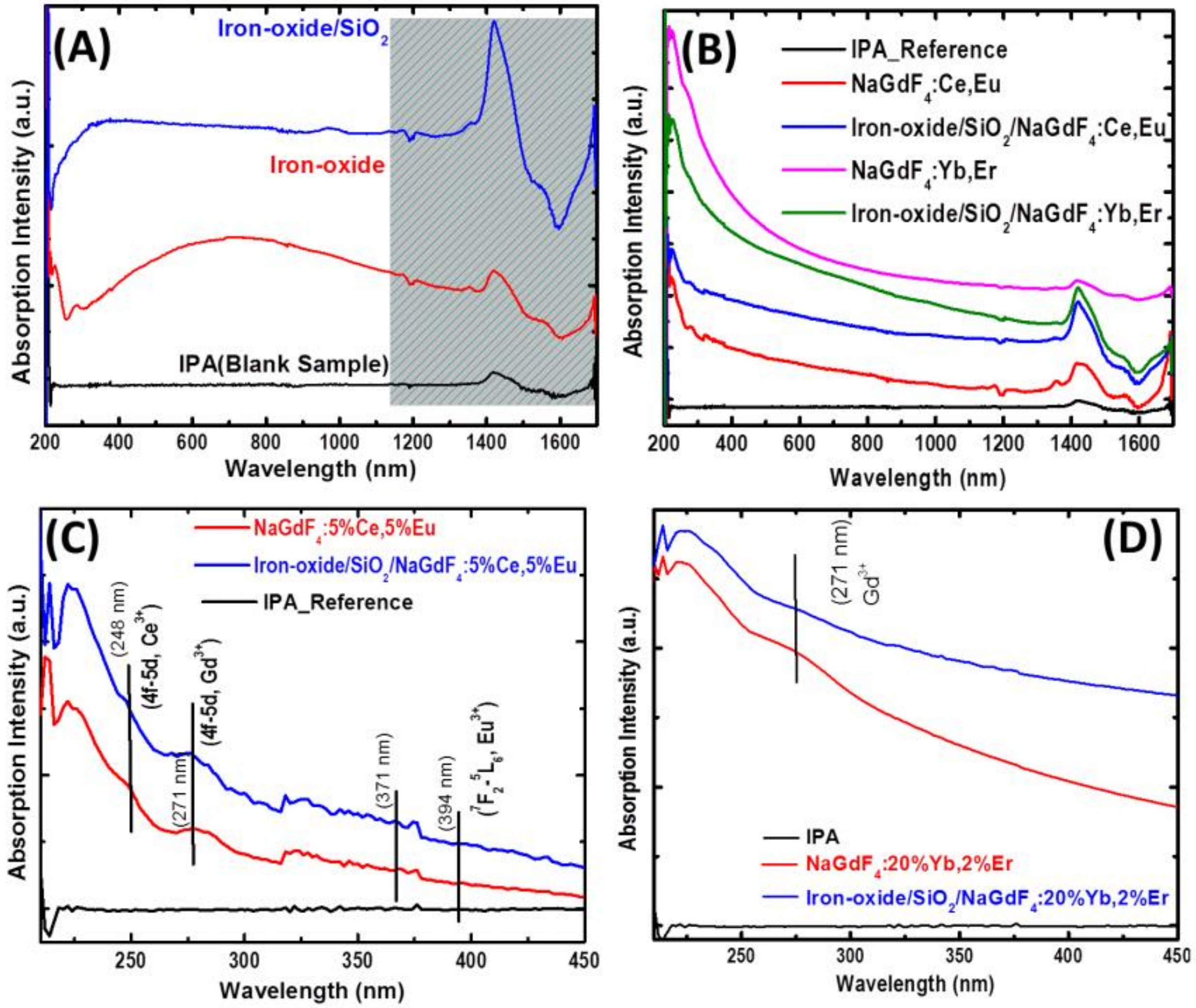

Figure E: UV-vis-NIR measurements in the range from 200 nm to 1700 nm of the samples (A) iron-oxide and iron-oxide/SiO_2; (B) $NaGdF_4$:RE (RE = Ce, Eu; Yb, Er) and Iron-oxide/SiO_2/$NaGdF_4$:RE, along with the reference sample (IPA); and extended absorption spectra of (D) Ce,Eu doped and (E) Yb, Er doped nanoparticles in the range 210 to 450 nm.

Generally, Fe_3O_4 is crystallized in the inverse spinel structure, where, Fe^{2+} and Fe^{3+} ions are distributed in the tetrahedral (T_d) and octahedral.(O_h) sites, as represented by structural formula: $[Fe^{3+}]T_d[Fe^{3+}Fe^{2+}]O_hO_4$. The Fe_3O_4 electronic structure shows only 3d energy states of iron ions near the

Fermi level so that the optical absorption due to electric–dipole induced transitions is not expected at optical frequencies by Laport's rule (parity forbidden). However, the diagonal components of the dielectric tensors of this compound obtained by optical measurements show strong absorption bands in the visible range. They are assigned to d–d intervalence charge transfer (IVCT) transitions in which a "*d*" electron of Fe^{2+} ion is transferred to the Fe^{3+} ion by optical excitation. [1,2]

The IVCT transitions occur between the iron ions of the octahedral site: $t_{2g}[Fe^{2+}]O_h \rightarrow e_g[Fe^{3+}]O_h$ (2.1 eV or 590 nm or 16937.64 cm^{-}), as well as from the Fe^{2+} of octahedral to the Fe^{3+} ion of tetrahedral site: $t_{2g}[Fe^{2+}]O_{h\rightarrow}e[Fe^{3+}]T_d$ (3.3 eV or 375 nm or 26616.16 cm^{-1}). Moreover, the $t_2[Fe^{3+}]T_d \rightarrow !t_{2g}[Fe^{3+}]O_h$ (2.6 eV, 476 nm or 20970 cm^{-1}) and $t_2[Fe^{3+}]T_d \rightarrow e_g[Fe^{3+}]O_h$ (4.0 eV or 309 nm, 32262.17 cm^{-1}) intersublattice charge-transfer (ISCT) transitions involve only trivalent oxidation state iron ions. A similar cation-to-cation charge transfer state is responsible for the color of the black magnetite or lodestone minerals.

Therefore, iron oxides act as luminescence quencher. This phenomenon occurs via an energy transfer process when a luminescent center (e.g., RE^{3+} ion) is directly in contact with or is in proximity to the iron oxide surface (e.g., Fe_3O_4). To overcome this disadvantage, the intermediate layer or spacer is usually added to separate the iron oxide nanoparticles and luminophores. Therefore, they are coated with organic macrocycles, polymers, silica, etc., to prepare the optical and magnetic nanomaterials. [3,4]

(F) Magnetic Investigation:

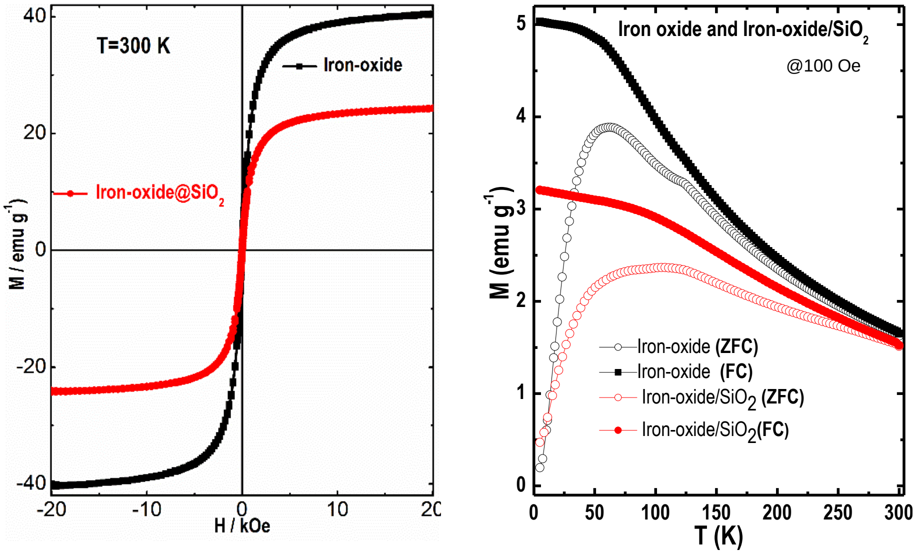

Figure S4(i) Hysterisis at 300 K (left panel) and zero field and field cooling (ZFC/FC) plots of of superparamagnetic iron oxide and iron-oxide/SiO$_2$.

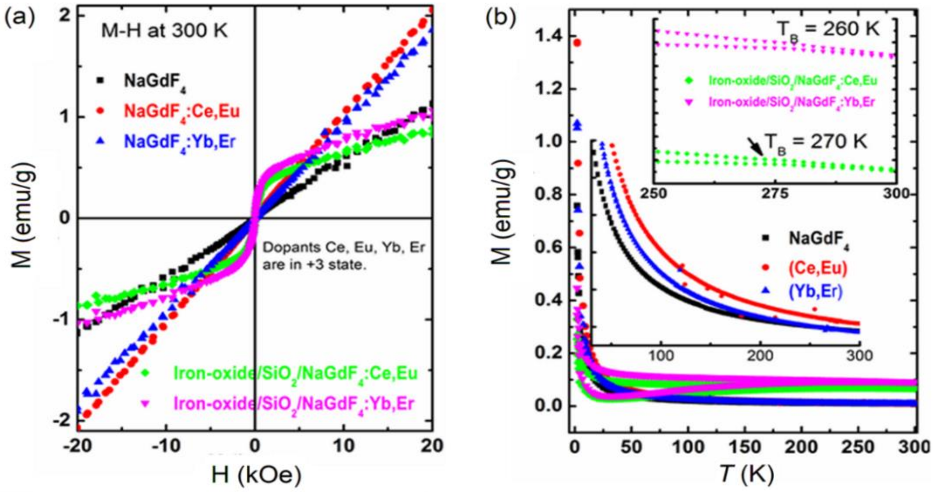

Figure S4(ii) (a) The magnetic hysteresis loops taken at 300 K, and (b) Zero field cooling and field cooling (ZFC/FC) magnetization versus temperature data at 100 Oe of NaGdF$_4$:RE (RE = Ce, Eu and Yb, Er) and iron-oxide/SiO$_2$/NaGdF$_4$:RE nanoparticles.

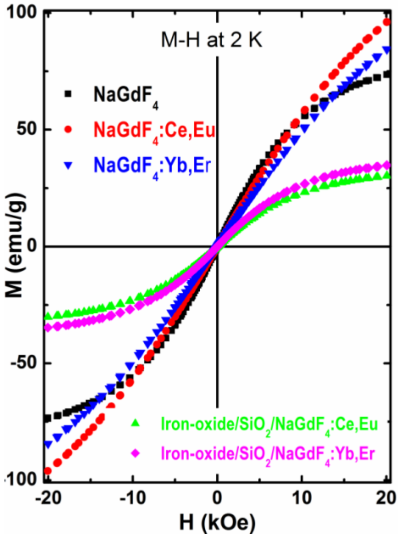

Figure S4 (iii): Hysterisis loops of samples at 2 K of NaGdF$_4$, NaGdF$_4$:RE and iron-oxide/SiO$_2$/NaGdF$_4$:RE (RE = Ce, Eu; Yb, Er).

(G) MRI Contrast Agents: Measurements conditions and details have been given in the manuscript in experimental section. All nanoparticles were dissolved in water. Results are reported as mean ± standard deviation.

Table T5 **T_2 values of NaGdF$_4$:RE^{3+} (RE = Ce, Eu; Yb, Er) nanoparticles**

samples	T_2 ± s.d. (ms)		
	0.0375 mM Gd	0.01875 mM Gd	0 mM Gd
NaGdF$_4$:5%Ce,5%Eu	577.7 ± 28.4 ms	831.7 ± 111.2 ms	–
NaGdF$_4$:20%Yb,2%Er	812 ± 47.9 ms	1213.3 ± 97.1 ms	–
water	–	–	2113.3 ± 338.4

Notes:

1. Iron oxide/SiO$_2$/NaGdF$_4$:5%Ce,5%Eu and iron oxide/SiO$_2$/NaGdF$_4$:20%Yb,2%Er nanoparticles have r_1 values that are on par with the clinically approved T_1 agents such as Gd-DOTA at this field strength.
2. Iron oxide/SiO$_2$/NaGdF$_4$:5%Ce,5%Eu has remarkably high r_2, significantly higher than the commercially available Feridex (39–43 mM^{-1}s^{-1}, 1.5 T).

Reference:

1 L. U. Khan and Z. U. Khan, in *Complex Magnetic Nanostructures*, Springer International Publishing, Cham, 2017, pp. 121–171.

2 L. U. Khan, H. F. Brito, J. Holsa, K. R. Pirota, D. Muraca, M. C. F. C. Felinto, E. E. S. Teotonio and O. L. Malta, *Inorganic Chemistry*, 2014, **53**, 12902–12910.

3 L. Tong, J. Shi, D. Liu and Q. Li, *The Journal of Physical chemistry C*, 2012, **116**, 7153–7157.

4 R. R. Silva, A. P. Duarte and R. M. Sa, *Chem Select*, 2016, 5923–5928.